npj | vaccines

Article

Published in partnership with the Sealy Institute for Vaccine Sciences

https://doi.org/10.1038/s41541-024-00947-4

A broad-spectrum vaccine candidate against H5 viruses bearing different sub-clade 2.3.4.4 HA genes

Yuancheng Zhang, Pengfei Cui, Jianzhong Shi, Xianying Zeng, Yongping Jiang, Yuan Chen, Jie Zhang, Congcong Wang, Yan Wang, Guobin Tian, Hualan Chen, Huihui Kong ✉ & Guohua Deng ✉

The global spread of H5 clade 2.3.4.4 highly pathogenic avian influenza (HPAI) viruses threatens poultry and public health. The continuous circulation of these viruses has led to their considerable genetic and antigenic evolution, resulting in the formation of eight subclades (2.3.4.4a–h). Here, we examined the antigenic sites that determine the antigenic differences between two H5 vaccine strains, H5-Re8 (clade 2.3.4.4g) and H5-Re11 (clade 2.3.4.4h). Epitope mapping data revealed that all eight identified antigenic sites were located within two classical antigenic regions, with five sites in region A (positions 115, 120, 124, 126, and 140) and three in region B (positions 151, 156, and 185). Through antigenic cartography analysis of mutants with varying numbers of substitutions, we confirmed that a combination of mutations in these eight sites reverses the antigenicity of H5-Re11 to that of H5-Re8, and vice versa. More importantly, our analyses identified H5-Re11_Q115L/R120S/A156T (H5-Re11 + 3) as a promising candidate for a broad-spectrum vaccine, positioned centrally in the antigenic map, and offering potential universal protection against all variants within the clade 2.3.4.4. H5-Re11 + 3 serum has better cross-reactivity than sera generated with other 2.3.4.4 vaccines, and H5-Re11 + 3 vaccine provided 100% protection of chickens against antigenically drifted H5 viruses from various 2.3.4.4 antigenic groups. Our findings suggest that antigenic regions A and B are immunodominant in H5 viruses, and that antigenic cartography-guided vaccine design is a promising strategy for selecting a broad-spectrum vaccine.

Influenza A virus threatens both the poultry industry and mammalian health. To date, 16 hemagglutinin (HA) and 9 neuraminidase (NA) subtypes have been found in aquatic birds[1,2], and two HA and two NA subtypes have been identified in bats[3,4]. In their reservoir species, most influenza virus subtypes are low pathogenic, although two subtypes (H5 and H7) have evolved into highly pathogenic strains[5]. The H5 highly pathogenic avian influenza viruses (HPAIVs), with a mortality rate close to 100% in chicken and turkey, have caused substantial economic losses to the global poultry industry. According to the OIE-World Animal Health Information System (OIE-WAHS, https://wahis.woah.org), the H5 HPAIVs have led to the loss of 389 million poultry[6]. In addition to this damage to poultry, the H5 virus also exhibits pandemic potential. As of January 5, 2024, the H5 AIVs have caused 969 human infections, including 495 deaths[7]. It is therefore imperative to develop strategies to control and prevent H5 subtype virus infections.

The antigenic drift and shift of influenza viruses necessitates frequent updates of vaccine strains, underscoring the need for broadly protective influenza vaccines. To expand the protection breadth of current vaccines, various strategies have been developed[8]. One such strategy is to combine multiple HA antigens. For example, a combination of three H1 HA immunogens improved the breadth of immunity against divergent H1 human influenza viruses[9], demonstrating the efficacy of multi-antigen strategies to achieve comprehensive immunity. Another innovative approach, to developing an H3 vaccine, incorporated scrambled immunodominant epitopes, and was proven effective in expanding coverage in ferret models. This was achieved by reducing the immunodominance of HA head epitopes, thereby enhancing the vaccine's protective range[10]. Moreover, a multivalent mRNA vaccine-induced protection against all 20 known influenza A virus subtypes and influenza B virus lineages in animals[11]. Another approach to generate broader subtype-specific

State Key Laboratory of Animal Disease Control and Prevention, Harbin Veterinary Research Institute, Chinese Academy of Agricultural Sciences, Harbin, China. ✉e-mail: konghuihui@caas.cn; dengguohua01@caas.cn

immune responses is through consensus sequences[12–17]. For example, Giles et al. reported a broadly reactive H5 antigen that was optimized by using a computational algorithm; the efficacy of this design to elicit broadly reactive antibodies was confirmed in animal models[14]. Although a range of creative and varied strategies have been employed, only a few will reach clinical trials, and the quest for a universal influenza vaccine remains a formidable challenge.

Understanding the mechanism of antigenic change is key to developing a vaccine. The antigenicity of influenza A viruses is mainly determined by the HA protein, especially its head region[18]. In the last century, five major antigenic epitopes have been identified in the head domain of HA by using mouse monoclonal antibodies (mAbs)[19–23]. The antigenicity of influenza viruses was found to be primarily determined by a few key amino acid substitutions around the receptor-binding site by characterizing antigenic variants with polyclonal antibodies[24–26]. In the head domain of HA, the amino acids at positions 129, 133, 151, 183, 185, and 189 (H5 numbering, used hereafter)[26], located at epitope sites A and B[27], were found to be the key determinants of the antigenicity of H5 viruses. Although mAbs can detect subtly differences between antigenic variants, polyclonal antisera, which correlate with host immune response, are used the most to evaluate the antigenic distance between virus isolates. Hemagglutinin inhibition (HI) and microneutralization (MN) assays are also used to evaluate antigenic characteristics; however, it is difficult to interpret raw HI and MN data. Accordingly, antigenic cartography was developed to analyze and visualize the relationships among multiple antigen–antibody reaction data pairs[25,28,29]. Benefiting from antigenic cartography, the WHO has used this tool to supplement influenza surveillance activities and guide vaccine strain selection[30].

HPAIVs of the H5 subtype have evolved into 10 different genetic clades (0–9) and many subclades. Notably, subclade 2.3.4.4 of the H5 viruses, first identified in poultry in 2013 and spread worldwide by migratory birds, has branched into eight subclades (2.3.4.4a to 2.3.4.4h)[31,32]. To control outbreaks of clade 2.3.4.4 H5 virus in 2015, China developed the first 2.3.4.4 H5N1 vaccine (designated as H5-Re8)[33], belonging to 2.3.4.4g clade[31]. Introduced by migratory birds, the new clade 2.4.4.4h emerged among China's poultry in 2018, presenting a considerable antigenic difference from the vaccine strain H5-Re8 and leading to the development of a new, antigenically matched vaccine designated H5-Re11[34]. In this study, we sought to identify the key amino acid substitution(s) that determine the antigenic difference between H5-Re8 and H5-Re11 by using antigenic cartography analysis. We identified eight antigenic sites that determine the antigenic difference between H5-Re8 and H5-Re11. In addition, we identified a promising vaccine seed strain bearing three mutations that seem to confer solid protection against all circulating clade 2.3.4.4 (a–h) viruses.

Results

Mapping of antigenic sites

The vaccine strain H5-Re8 contains surface genes from a clade 2.3.4.4g virus, A/chicken/Guizhou/4/13(H5N1) (GZ/4/13), and six internal genes from the high-growth A/Puerto Rico/8/1934 (H1N1) (PR8) virus. It differs antigenically from the H5-Re11 strain that harbors surface genes from a clade 2.3.4.4h virus, A/duck/Guizhou/S4184/2017(H5N6) (GZ/S4184/17), and internal genes from PR8[34]. Sequence analysis indicates that there are 20 amino acid differences in HA1 between these two vaccines (Fig. 1).

To elucidate which amino acid substitution(s) determines this antigenic difference, we used reverse genetics to rescue 20 H5-Re11 mutants. Firstly, we evaluated the growth properties of the mutants and then analyzed their antigenicity by using a HI assay with H5-Re8 and H5-Re11 antisera. As shown in Table 1, none of the mutations had an adverse effect on the growth properties; all the mutants grew to relatively high titers (Table 1). To our surprise, none of the substitutions changed the antigenicity of the mutants in the HI assay, except mutant H5-Re11_−126D (−, an amino acid deletion at position 126), which showed higher titer with H5-Re8 antiserum, with an HI titer that was 2-fold higher than that of the other mutants (Table 1). To distinguish the subtle antigenic difference, a panel of 19 mAbs was generated and used to evaluate the antigenicity of the mutants. The 19 mAbs identified seven mutants that displayed considerable antigenic differences in the HI assay (i.e., at least a 4-fold difference), namely H5-Re11_Q115L, H5-Re11_R120S, H5-Re11_N124D, H5-Re11_V140M, H5-Re11_T151I, H5-Re11_A156T, and H5-Re11_E185A (Fig. 2). Thus, eight antigenic sites in H5 HA, 115, 120, 124, 126, 140, 151, 156, and 185, were identified.

Molecular basis of the antigenic difference between H5-Re8 and H5-Re11

We next investigated which combination of antigenic substitutions changed the antigenicity of H5-Re11 to that of H5-Re8 or vice versa. First, we categorized the eight antigenic positions into three groups: Group 1 containing positions 115, 120, and 156, which were the three positions that most

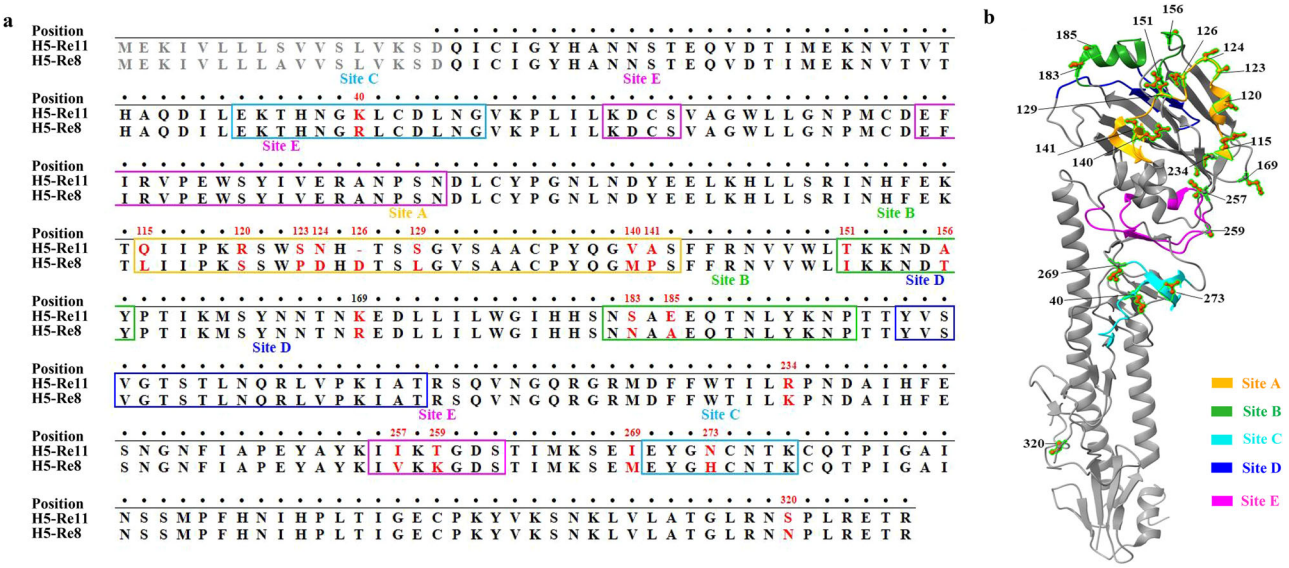

Fig. 1 | Key amino acid alterations in the HA proteins of H5 viruses. a Alignment of HA1 protein sequences (H5 numbering). Antigenic regions A, B, C, D, and E are delineated and highlighted in orange, green, cyan, blue, and pink, respectively. Sites with amino acid variations are marked and highlighted in red. **b** The site exhibiting amino acid variation is depicted in the HA monomer of an H5 virus, retrieved from the PDB database (5HUF). Amino acid substitutions at antigenic sites are denoted in red, and the respective antigenic regions are marked with corresponding colors.

Table 1 | Cross-reactive HI antibody titers of mutant viruses with different antisera

Virus (H5 numbering)	Serum		Virus titer	
	H5-Re8	H5-Re11	EID_{50}/ml	HA (log_2)
Re8	2048	64	8.63	8
Re11	256	256	8.63	8
Re11_K40R	256	256	8.17	7
Re11_Q115L	256	256	8.83	8
Re11_R120S	256	256	8.83	8
Re11_S123P	256	256	8.63	8
Re11_N124D	256	256	8.63	8
Re11_-126D	512	256	8.17	8
Re11_S129L	256	256	8.63	8
Re11_V140M	256	256	8.50	7
Re11_A141P	256	256	9.17	8
Re11_T151I	256	256	8.83	8
Re11_A156T	256	256	9.17	8
Re11_K169R	256	256	9.17	7
Re11_S183N	256	256	8.63	8
Re11_E185A	256	256	9.17	8
Re11_R234K	256	256	9.17	8
Re11_I257V	256	256	8.17	8
Re11_T259K	256	256	8.83	8
Re11_I269M	256	256	8.83	8
Re11_N273H	256	256	8.17	8
Re11_S320N	256	256	8.83	8

"–" An amino acid deletion at position 126 (H5 numbering).

changed the antigenicity of H5-Re11 (Fig. 2); Group 2 containing positions 140, 151, and 185, which changed the antigenicity of H5-Re11 to a lesser extent (Fig. 2); and Group 3 containing positions 124 and 126, which affected the antigenicity of H5-Re11 and resulted in the formation of a glycosylation site (Table 1 and Supplementary Fig. 1). Then, three mutants, H5-Re11_Q115L/R120S/A156T (H5-Re11 + 3), H5-Re11_Q115L/R120S/V140M/T151I/A156T/E185A (H5-Re11 + 6), and H5-Re11_Q115L/R120S/N124D/-126D/V140M/T151I/A156T/E185A (H5-Re11 + 8) were rescued by gradually adding groups of mutations into the H5-Re11 vaccine strain. Their antigenicity was analyzed by using the HI assay with chicken sera generated with one clade 2.3.4.4b virus, one clade 2.3.4.4g virus, and two 2.3.4.4h viruses that were antigenically different. Antigenic cartography showed that the antigenicity of mutant H5-Re11 + 8 was closest to that of GZ/4/13 (donor virus of H5-Re8), whereas mutants H5-Re11 + 6 and H5-Re11 + 3 were still antigenically different from GZ/4/13 (Fig. 3a and Supplementary Table 1). To confirm that the antigenic transition was caused by the mutations, a H5-Re8 mutant with eight corresponding mutations, H5-Re8_L115Q/S120R/D124N/D126-/M140V/I151T/T156A/A185E (H5-Re8 + 8), was generated and its antigenicity was evaluated. As expected, the antigenicity of H5-Re8 + 8 was similar to that of both H5-Re11 and GZ/S4184/17 (donor virus of H5-Re11) (Fig. 3a and Supplementary Table 1). Compared with the HI assay, the MN assay is considered the gold standard for the analysis of the antigenic properties of the viruses. Thus, the antigenicity of the mutants was further confirmed by the MN assay (Supplementary Table 2). Although the antigenic map generated with the HI data differed from that generated with the MN data (Fig. 3b), the MN map confirmed that the antigenic transition between H5-Re11 and H5-Re8 was caused by substitutions at the eight antigenic sites.

Selection of a broad-spectrum vaccine candidate based on antigenic distance

Since the implementation of the first clade 2.3.4.4g vaccine (H5-Re8) in 2015, three more vaccines, H5-Re11 (2.3.4.4h), H5-Re13 (2.3.4.4h), and H5-Re14 (2.3.4.4b), were generated to control clade 2.3.4.4 antigenic

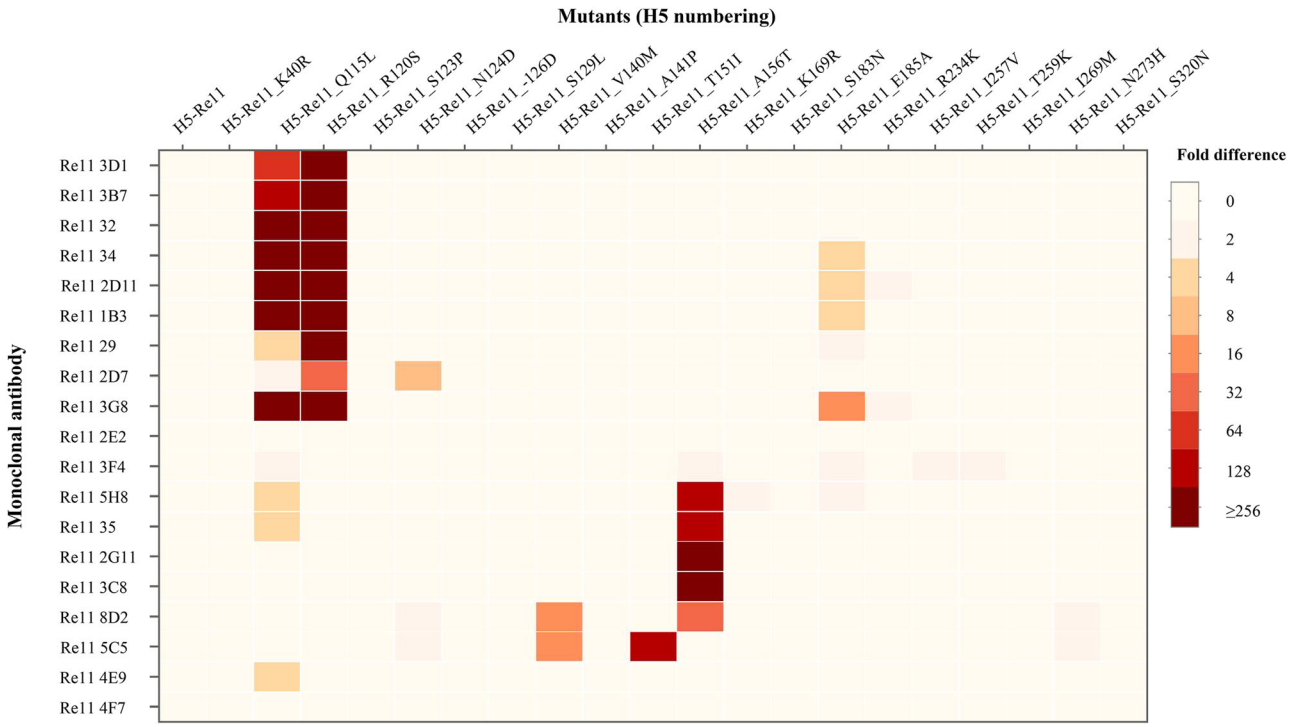

Fig. 2 | Antigenic heat map of H5-Re11 mutants. The antigenicity of the H5-Re11 variants was determined by quantifying HI titers utilizing a panel of 19 mAbs generated in our laboratory. A 4-fold difference in antigenicity was deemed significant.

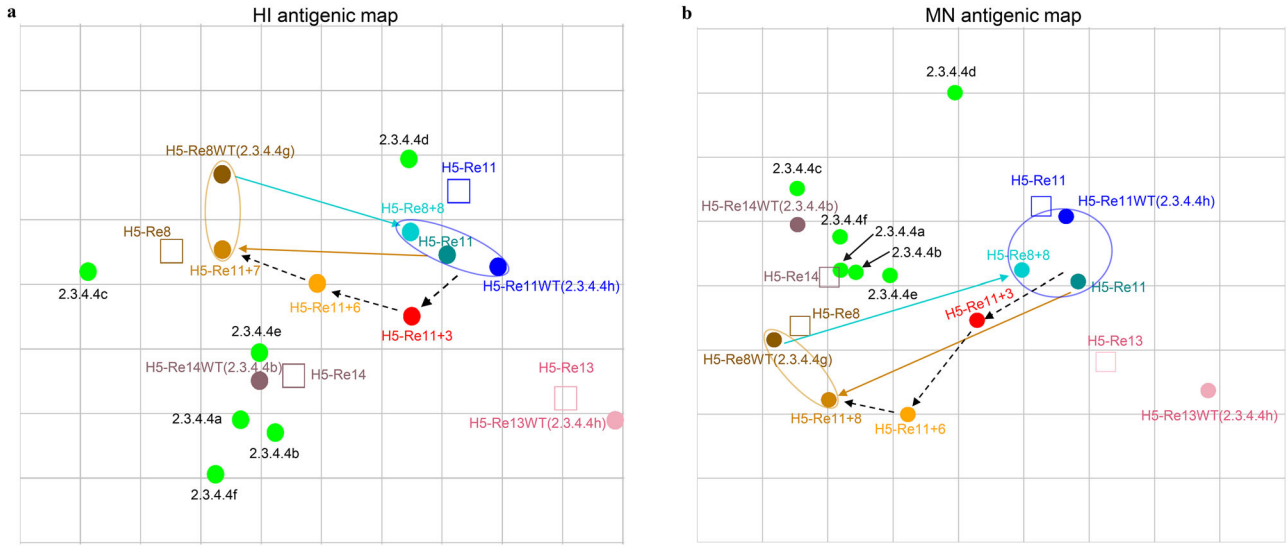

Fig. 3 | Antigenic cartography of the indicated mutants and reference viruses. a Antigen map constructed using HI titer data. **b** Antigen map generated based on MN titers. Each square represents a 2-fold difference in either HI or MN titers. Viruses and serum samples are represented by circles and rectangles, respectively.

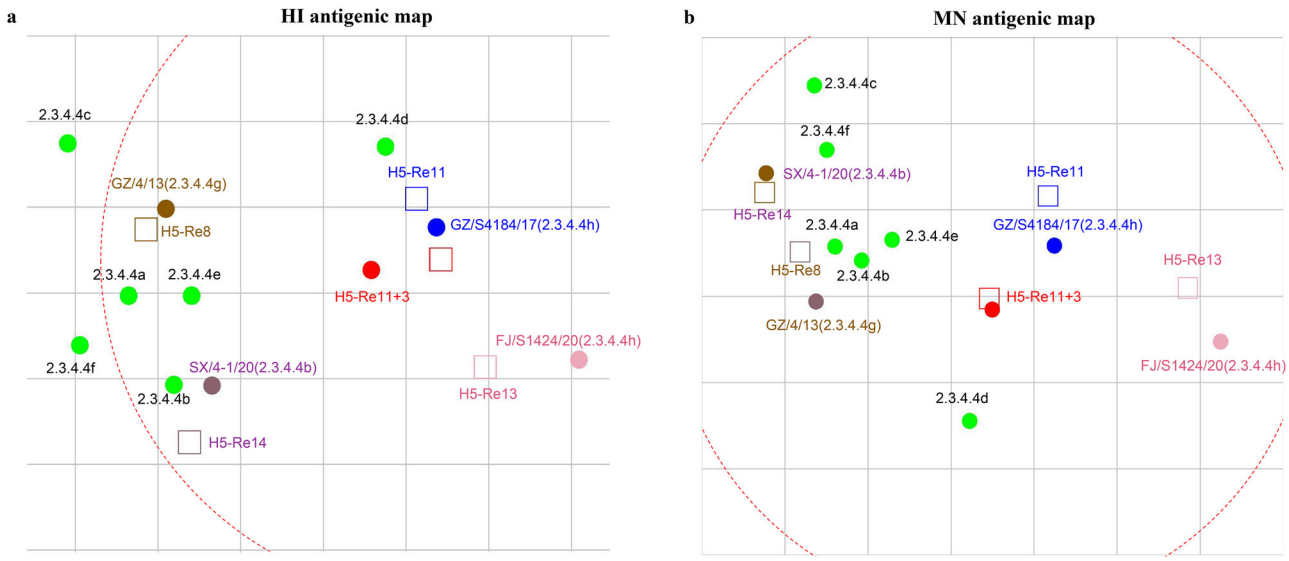

Fig. 4 | Protective breadth of serum generated with the Re11 + 3 mutant. a The scope of protective efficacy depicted in the antigenic map was constructed using HI titer data. **b** The scope of protective efficacy illustrated in the antigenic map was created with MN titer data. Each square represents a 2-fold difference in either HI or MN titers. Viruses and serum samples are represented by circles and rectangles, respectively. The dashed red circle on the map marks the region where the titers of the H5-Re11 + 3 serum fall below the thresholds of 32 or 64 for the HI and MN titers, respectively.

variants in China[34–36]. The frequent updating of vaccine strains highlights the need to develop a vaccine strain with broader protective efficacy. Our antigenic cartography analysis revealed that the mutant H5-Re11 + 3 was located in the relative center of the map, indicating its potential to serve as a broad-spectrum vaccine candidate against H5 viruses bearing the clade 2.3.4.4 HA gene. To evaluate the protective breath of H5-Re11 + 3, homologous serum of H5-Re11 + 3 was generated and applied for antigenic analysis with all eight subclades of 2.3.4.4 viruses (2.3.4.4a–h). In the HI assay, viruses in subclades 2.3.4.4a, 2.3.4.4c, and 2.3.4.4f reacted poorly with the H5-Re11 + 3 serum, with an HI titer of 16, whereas the HI titer of H5-Re11 + 3 against viruses in other subclades was 32–512 (Supplementary Table 3). In the antigenic map generated with the HI data, the breadth of the H5-Re11 + 3 serum response was calculated as described by Ron et al. (Fig. 4a)[37]. The H5-Re11 + 3 serum covered viruses in six subclades of 2.3.4.4, except 2.3.4.4c and 2.3.4.4f, which have not circulated since 2019 and 2017, respectively[38,39] (Supplementary Fig. 2). We also evaluated the protective efficacy by using the MN assay, the gold standard for evaluating a vaccine's protective capabilities. Notably, the data indicated that H5-Re11 + 3 serum reacted well with viruses in all eight subclades, with MN titers ranging from 64 to 1028, above the typical protective value (titers > 40) (Supplementary Table 4). As expected, in the antigenic map generated with the MN data (Fig. 4b), H5-Re11 + 3 serum was found to be located in the relative center of the antigenic map, and its breadth covered all eight subclades of the 2.4.4.4 viruses. Together, these data suggest that H5-Re11 + 3 is a potential broad-spectrum vaccine candidate against viruses belonging to clade 2.3.4.4.

Protective efficacy of H5-Re11 + 3 inactivated vaccine against clade 2.3.4.4 viruses

Lastly, we assessed the protective efficacy of the H5-Re11 + 3 vaccine in chickens that were immunized with a single dose of the inactivated H5-Re11 + 3 vaccine. The chickens were then challenged with clade 2.3.4.4 antigenic variants that previously caused epidemics in poultry: one 2.3.4.4g virus, one 2.3.4.4b virus, and two 2.3.4.4h viruses belonging to two different antigenic groups (Fig. 4). The antigenic map (Fig. 4) indicated that H5-Re11 serum may confer relatively broad protection against other clade viruses. Therefore, vaccine strain H5-Re11 was used for comparison in the challenge study. The H5-Re11 + 3- inactivated vaccine was immunogenic in chickens; three weeks after the single dose, the mean HI titer in chickens against the homologous virus was 7.4 $\log_2$, which is 0.3 $\log_2$ higher than that of the H5-Re11 vaccine (Fig. 5a, d, g, and j).

The H5-Re8 vaccine was used to control clade 2.3.4.4g viruses between 2015 and 2018 and provided full protection against GZ/S4184/17 (clade 2.3.4.4h), which emerged in 2017[6]. In the GZ/4/13 (clade 2.3.4.4g) virus-challenged group, the H5-Re11 + 3 vaccine induced a significantly higher HI titer against GZ/4/13 than that induced by H5-Re11 (Fig. 5a). All chickens in the control groups died within 4 days post-challenge (p.c.), and the two chickens that survived on day 3 p.c. shed high titers of viruses through both the oropharynx and cloaca (Fig. 5b, c). In the H5-Re11-vaccinated group, 60% of the birds died during the 14-day observation period, and all the birds shed virus in the oropharynx and cloaca on days 3 and 5 p.c., except for one chicken that died on day 7 post-immunization (p.i). However, in the H5-Re11 + 3-vaccinated group, no virus was recovered from the organs, and all the vaccinated birds were healthy during the 14-day observation period (Fig. 5b, c). These data indicate that H5-Re11 provides only partial protection against the 2.3.4.4g virus, whereas H5-Re11 + 3 offers complete protection against the same virus.

The H5-Re11 vaccine was used to control clade 2.3.4.4h viruses between 2018 and 2021[6]. In the GZ/S4184/17 (clade 2.3.4.4h) virus-challenged group, the H5-Re11 + 3 vaccine induced a similar HI titer against GZ/S4184/17 to that induced by H5-Re11 (Fig. 5d). All chickens in the control groups died, and the three chickens that survived on day 3 p.c. shed high titers of viruses in collected organs. In the H5-Re11 + 3 and H5-Re11-vaccinated groups, no virus was recovered from the organs, and all the vaccinated birds were healthy during the 14-day observation period (Fig. 5e, f). These data demonstrate that H5-Re11 + 3, despite harboring three mutations, provides 100% protection against the GZ/S4184/17 virus.

The H5-Re13 vaccine was used instead of H5-Re11 to control antigenic variants in clade 2.3.4.4h, beginning in 2022[6]. In the A/duck/Fujian/S1424/2020(H5N6) (FJ/S1424/20, donor virus of H5-Re13) virus-challenged groups, the H5-Re11 + 3 vaccine induced a significantly higher HI titer against FJ/S1424/20 than that induced by H5-Re11 (Fig. 5g). All chickens in the control groups died, and the three chickens that survived on day 3 p.c. shed high titers of viruses in collected swabs. In the H5-Re11-vaccinated group, all the chickens survived the 14-day observation period, but they all shed viruses in the two tested organs on day 3 p.c., while 8 and 4 chickens shed viruses in the oropharynx and cloaca swabs, respectively, on day 5 p.c. In contrast, all the chickens in the H5-Re11 + 3-vaccinated group were healthy and shed no virus for 14 days (Fig. 5h, i). These results show that H5-Re11 mitigates lethality but fails to prevent virus shedding after FJ/S1424/20 challenge, whereas H5-Re11 + 3 affords comprehensive protection against the virus.

The H5-Re14 vaccine was used to control clade 2.3.4.4b virus, beginning in 2020[6]. In the A/whooper swan/Shanxi/4-1/2020(H5N8) (SX/4-1/20, donor virus of H5-Re14) virus-challenged group, the H5-Re11 + 3 vaccine induced a significantly higher HI titer against SX/4-1/20 than that induced by H5-Re11 (Fig. 5j). Chickens in the control group all died within 4 days p.c., and the surviving birds shed viruses to high titers. In the H5-Re11-immunized group, no chicken died and no virus was shed in the cloaca swabs; however, the virus was detected in oropharyngeal swabs from 4 chickens on days 3 and 5 p.c. For chickens immunized with the H5-Re11 + 3 vaccine, no virus was detected in the tested swabs, and no symptoms were observed for 14 days (Fig. 5k, l). These data indicate that H5-Re11 + 3 offers 100% protection against the 2.3.4.4b virus.

Taken together, these results indicate that the H5-Re11 + 3 vaccine provides solid protection against four antigenically drifted clade 2.3.4.4 H5 viruses.

Discussion

In this study, we mapped the antigenic sites of H5 HPAIVs, leading to the discovery of a vaccine candidate that is stable in chicken embryonated eggs for at least five passages (data not shown) and offers broad-spectrum protection against clade 2.3.4.4 viruses. Analysis of the antigenic differences between H5-Re8 and H5-Re11 revealed that these differences arise due to substitutions at eight antigenic sites. These substitutions—Q115L, R120S, N124D, −126D, V140M, T151I, A156T, and E185A−-result in H5-Re11 having antigenic properties similar to those of H5-Re8, and vice versa. Antigenic cartography placed H5-Re11 + 3 centrally on the antigenic map, indicating its antigenic similarity to neighboring viruses. Further studies, including antigenic analysis and protective efficacy testing, confirmed its broad-spectrum efficacy against all viruses within the 2.3.4.4 clade. Our results suggest that vaccine design guided by antigenic cartography is a promising strategy for the development of broad-spectrum vaccines.

Five major antigenic regions (A–E) have been identified through the characterization of escape mutants from mouse mAbs directed at the HA of human influenza A viruses[20,22,23,40]. For human H3N2 viruses, antigenic region B has been shown to be immunodominant over antigenic region A in both humans and mice[27,41,42]. Similarly, the antigenic region B of HA plays a critical role in the antigenic drift of subclade 2.3.4.4 H5 HPAIVs[43]. However, computational analysis has revealed that antigenic regions A and B have the largest average information entropy, indicating that they are under the highest immune pressure[44]. In our study, the epitope mapping data revealed that all eight identified antigenic sites were located within two classical antigenic regions, with five in antigenic region A (115, 120, 124, 126, and 140) and three in antigenic region B (151, 156, and 185). Consistent with our data, multiple studies have shown that both antigenic regions A and B play a critical role in the antigenic evolution of H5 viruses[45–48]. Kaverin et al. identified nine antigenic sites in the HA of A/mallard/Pennsylvania/10218/84 (H5N2), including seven positions in antigenic region A (124, 126, 129, 136, 138, 140, and 141) and two positions in antigenic region B (152 and 153)[48]. Rudneva et al. identified 10 antigenic sites in A/duck/Novosibirsk/56/05 (H5N1), including nine sites (113, 115, 117, 118, 120, 121, 123, 139, and 141) in antigenic region A and one site (162) in antigenic region B[46]. Position 126 in antigenic region A, which is involved in the formation of a glycosylation site, is the only antigenic site that could be recognized by the HI assay in our study, indicating its important role in viral antigenicity. Gu et al. reported that the E126N mutation creates an N-linked glycosylation site and results in an antigenic change in A/chicken/Hebei/A/2012(H5N2). Wang et al. reported that the D124N mutation results in the formation of a glycosylation site at site 126 and antigenic changes in H5N6 viruses[49]. However, the role of antigenic site 156, another site involved in the formation of a glycosylation site in antigenic region B, has only been recognized by mAbs and not polyclonal antibodies (Table 1 and Supplementary Fig. 1), indicating that antigenic region A may be immunodominant in certain H5 viruses.

Diverging from other methods used to develop broad-spectrum vaccines, our approach involved selecting a candidate that offers more extensive protection. This choice was guided by antigenic cartography, based on the hypothesis that a virus positioned centrally in an antigenic map would exhibit the greatest range of immunity. Similarly, Hu et al. reported that a booster vaccine (SARS-CoV-1) selected based on antigenic distance outperforms other candidates to elicit broader neutralizing responses against SARS-CoV-2 variants[50]. In our study, the H5-Re11 + 3 vaccine was identified during the antigenic analysis of clade 2.3.4.4 viruses; however, the mechanism of how to relocate the antigenic position of a vaccine strain to the relative center position of the antigenic map remains to be investigated. Although the HI assay has been the most commonly used serological assay

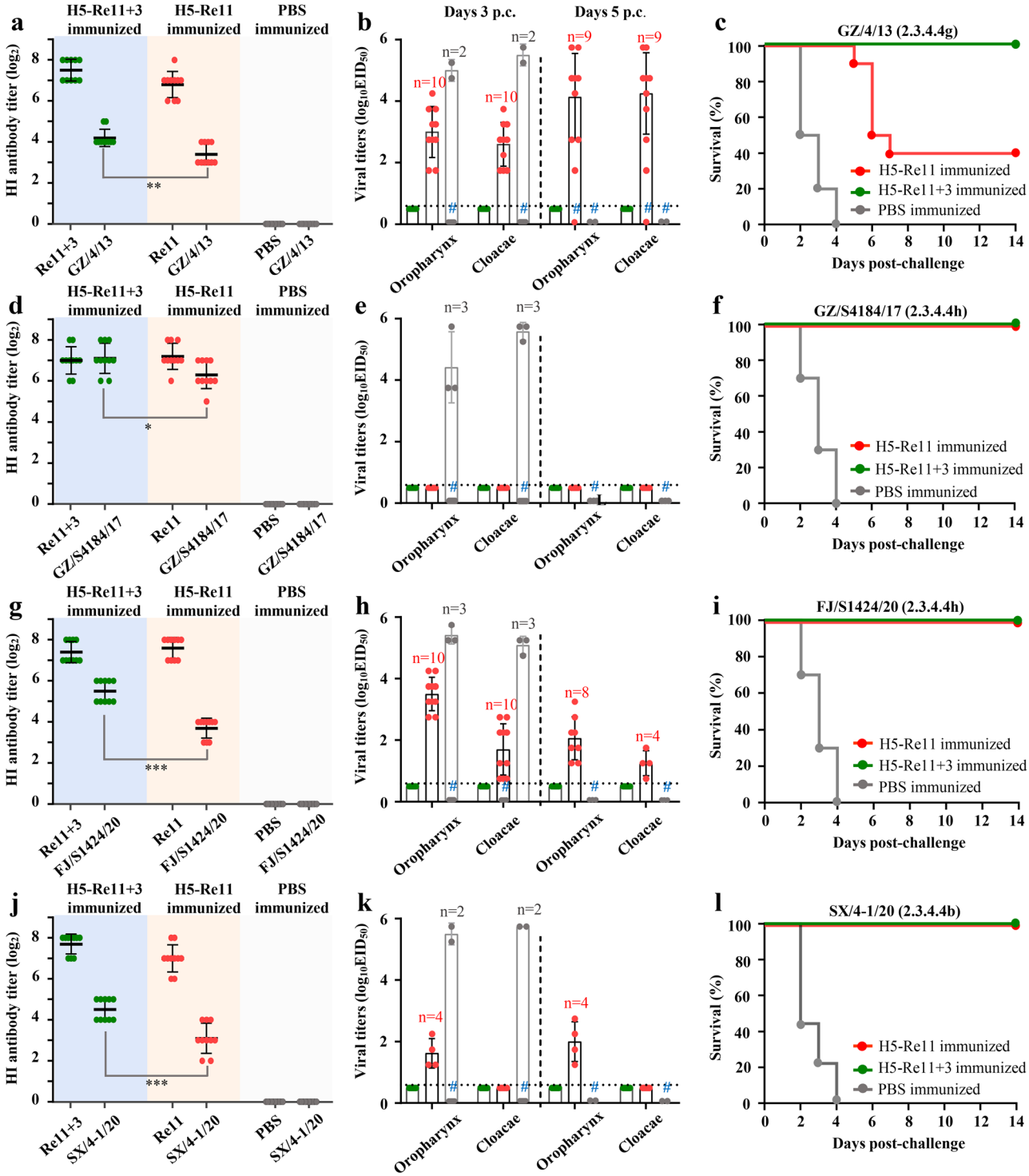

Fig. 5 | Evaluation of the protective efficacy of H5-Re11 + 3 vaccine against clade 2.3.4.4 viruses in chickens. Groups of birds were administered either the H5-Re11 + 3 vaccine, the Re11 vaccine, or a PBS control. Three weeks post-immunization, sera were collected from all experimental chickens and analyzed for HI antibody titers against both the vaccine strain and the challenge virus (**a**, **d**, **g**, and **j**). To assess virus shedding, oropharyngeal and cloacal swabs were collected from all surviving chickens on days 3 and 5 post-challenge (**b**, **e**, **h**, and **k**). Subsequently, all the chickens were challenged with 10^5 EID_{50} of the indicated virus in a 100-μl volume of PBS. Following the challenge, chickens were monitored for two weeks to observe signs of disease progression and mortality (**c**, **f**, **i**, and **l**). Virus titers presented are the mean values derived from the birds that survived, with error bars indicating the standard deviations. The blue pound symbols denote the instances where birds died before the specified day. In cases where fewer than ten birds survived, the exact number of survivors is noted. The dashed lines represent the lower limit of virus detection. Statistical significance ($p < 0.05$) was determined by using GraphPad software, utilizing an unpaired *t*-test method for the analysis.

to assess virus antigenicity, HI titer and protective efficiency against H5 viruses are not strictly correlated[51,52]. As a result, the protective breadth of H5-Re11 + 3, which completely prevented death and virus shedding in chickens (Fig. 5), was not fully represented in the antigenic cartography generated with the HI data (Fig. 4a), but was perfectly exhibited in the antigenic map generated with the MN data (Fig. 4b).

Cao et al. demonstrated that a mAb against H5N1 virus AFluIgG01 that targets three sites on the membrane-distal globular head of HA1 [Site I (Ile116, Ile117, and Pro118), site II (Trp122 and Ser123) and site III (Tyr164 and Thr167)] can inhibit virus-receptor binding and pH-induced, cell-cell membrane fusion[53]. Given that two of the mutations of H5-Re11 + 3, namely Q115L, and R120S, are located close to sites I and II identified by Cao et al., it is reasonable to speculate that the H5-Re11 + 3 vaccine may elicit antibodies that recognize conformational epitope(s) that result in broad protection. The mechanism that induces such broad protection remains to be investigated.

In summary, our epitope mapping study identified eight antigenic sites of the H5 virus, and our antigenic analysis found a broad-spectrum vaccine candidate (H5-Re11 + 3) that conferred full protection against multiple subclades of 2.3.4.4 H5 viruses. Our study demonstrated that antigenic cartography-guided vaccine design is a promising strategy for selecting a broad-spectrum vaccine. Further antigenic analysis may identify additional vaccine candidates with broader protection.

Materials and methods

Biosafety and animal welfare

The animal experiment protocols were approved by the Committee on the Ethics of Animal Experiments (220706-01-GJ and 220815-02-GJ) at the Harbin Veterinary Research Institute (HVRI) of the Chinese Academy of Agricultural Sciences (CAAS). All animal experiments were carried out under Biosafety Level 3 (BSL3) conditions. Experiments involving HPAIVs were conducted in the BSL3 laboratory, whereas those involving LPAIVs were performed in the BSL2 laboratory.

Viruses and cells

Viruses A/duck/Chongqing/S1049/2014(H5N6) (2.3.4.4a), A/duck/Zhejiang/S4143/2017(H5N6) (2.3.4.4b), A/whooper swan/Shanxi/4-1/2020(H5N8) (SX/4-1/20, 2.3.4.4b), A/duck/Zhejiang/S1327/2016(H5N6) (2.3.4.4c), A/chicken/Jiangxi/5/2016(H5N6) (2.3.4.4d), A/chicken/Hunan/6/2015 (H5N6) (2.3.4.4e), A/chicken/Hunan/1/2016(H5N6) (2.3.4.4f), A/chicken/Guizhou/4/2013(H5N1), (GZ/4/13, 2.3.4.4g), A/duck/Guizhou/S4184/2017(H5N6), (GZ/S4184/17, 2.3.4.4h), and A/duck/Fujian/S1424/2020(H5N6) (FJ/S1424/20, 2.3.4.4h) were isolated during routine surveillance (GISAID Accession Numbers: EPI3279858, EPI3279859, EPI3279860, EPI3279861, EPI3279862, EPI3279863, EPI1921590, EPI_ISL_202553, EPI3279864, and EPI3279865). H5 vaccine strains H5-Re8, H5-Re11, H5-Re13, and H5-Re14, with the surface genes from GZ/4/13, GZ/S4184/17, FJ/S1424/20, and SX/4-1/20, respectively, developed in the backbone of PR8 were maintained in our laboratory[34–36]. Mouse myeloma cells (Sp2/0) and human embryonic kidney cells (293T) were cultured in DMEM medium supplemented with 10% fetal bovine serum (FBS). Madin-Darby canine kidney (MDCK) cells were cultured in a DMEM medium containing 5% FBS. All cell lines were incubated at 37 °C in a 5% CO_2 atmosphere.

Production and purification of mAbs

mAbs were generated by using the hybridoma technique as previously described[54]. In brief, 6-week-old female BALB/c mice received intramuscular injections containing 50 μg of the pCAGGS vector, which facilitates the expression of the H5-Re11WT HA protein, suspended in 200 μl of phosphate buffered saline (PBS). The mice were boosted twice with 10 μg of inactivated Re11 vaccine with a two-week interval between boosts. Hybrid cells were generated by the fusion of Sp2/0 myeloma cells and antibody-secreting cells. The positive hybridoma cells were identified by using the HI assay, and then monoclonal hybridoma cells (1.0×10^4 per mouse) were intraperitoneally injected into BALB/c mice sensitized with Freund incomplete adjuvant (500 μl per mouse). To quantify the mAbs, ascites antibodies from mice were purified by using a protein G affinity column (GE Healthcare, USA), and the concentration of the mAbs was measured by using a BCA protein assay kit (Bevotime. China).

Construction of recombinant mutant virus

In this study, the mutants were rescued with an avirulent HA gene featuring specified amino acid substitutions, along with the remaining gene segments from PR8. Initially, the HA gene from HPAIV was rendered avirulent by modifying the HA cleavage site, which contains multiple basic amino acids, to include only one basic amino acid—a characteristic typical of LPAIV. The recombinant viruses were then rescued using reverse genetics, as previously described[55]. In brief, 293T cells were seeded in a 6-well plate one day prior to transfection. Following the manufacturer's instructions, the cells were transfected with 4 μg of eight DNA plasmids (approximately 0.5 μg per plasmid) using Lipofectamine® LTX (Invitrogen, USA). After 10 h, the medium was replaced with Opti-MEM containing 0.125 μg/ml TPCK-trypsin (Sigma, USA). The cells were then incubated for 48 h at 37 °C and 5% CO_2 before harvesting the supernatant. To propagate the virus stocks, embryonated chicken eggs were inoculated with the supernatant from the transfected cells. After a 48 h incubation at 37 °C, the allantoic fluid was harvested, and the presence of introduced mutations, as well as the absence of any unwanted additional mutations, was confirmed through sequencing.

HI and MN assays

In accordance with methods delineated in previous studies[56], HI assays were conducted using a panel of chicken antisera or mAbs as previously described[56]. Sera or mAbs were mixed with 25 μl of PBS that contained four hemagglutinating units of the indicated virus. The resulting mixture was then maintained at room temperature for 20 min. Then, 25 μl of 1% chicken erythrocytes was added to the mixture, which was incubated for an additional 20 min. The titers were recorded and expressed as the reciprocal value of the highest dilution of serum that completely inhibited the agglutination of the chicken erythrocytes.

The MN assay was conducted as previously described[56]. Briefly, the serum was serially diluted 2-fold using DMEM medium supplemented with 1 mg/mL TPCK-trypsin. Then, 50 μl of the serially diluted serum was mixed with 50 μl of DMEM medium containing 100 50% tissue culture infectious dose ($TCID_{50}$) of the indicated virus and incubated at 37 °C for 1 h. The mixture was then transferred onto MDCK cells in 96-well plates, and the cells were cultured at 37 °C for 2 days. The MN titer is the highest dilution that inhibited virus replication.

Western blotting

The glycosylation patterns of HA proteins were assessed through Western blot analysis. Briefly, the viruses were purified through ultracentrifugation on a 30% sucrose cushion at 28,000 rpm for 90 min. Then, the viruses were diluted with PBS and stored at −80 °C for further analysis. For Western blotting, the viruses were lysed with NP-40 buffer containing Halt Protease Inhibitor Cocktail for 30 min at 4 °C. The presence of protein bands was determined using the Odyssey infrared imaging system, following incubation with Re-11 chicken anti-sera and an IRDye™ 700DX-conjugated secondary antibody.

Antigenic cartography

The antigenicity distances between viruses were assessed at https://www.antigenic-cartography.org/, as previously described[25,57]. The HI or MN titers were subjected to mathematical transformation to generate a comprehensive table delineating antigenic distances. This

transformation was conducted using the equation $D_{ij} = b_j - log_2 (H_{ij})$, where H_{ij} represents the titer corresponding to antigen i reacting against serum j, b is the log of the peak titer identified in reactions with serum j, and D_{ij} is the target distance between virus i and serum j. Subsequently, to optimize the representation, the error function represented as $(D_{ij} - d_{ij})^2$ was minimized, with d_{ij} denoting the Euclidean distance between two respective points delineated on the map.

Chicken study

To make an inactivated vaccine, 10 ml of the indicated virus was diluted with PBS to contain 7 log2 HA units in a volume of 50 μl, and then thoroughly mixed with 20 ml of oil adjuvant in a vaccine-generating machine. To evaluate the protective efficacy of the indicated vaccine strain against four viruses, GZ/4/13 (2.3.4.4g), GZ/S4184/17 (2.3.4.4h), FJ/S1424/20 (2.3.4.4h), and SX/4-1/20 (2.3.4.4b), a total of 120 chickens were used. Groups of 30 three-week-old White Leghorn specific pathogenic free chickens (hen) were injected intramuscularly with one dose (0.3 ml) of H5-Re11, H5-Re11 + 3, or PBS (10 chickens each, randomly selected). Three weeks post-vaccination (p.v.), serum samples were collected from all experimental chickens and assessed for HI antibody titers against both the vaccine strain and the challenge virus. Subsequently, ten chickens, immunized with H5-Re11, H5-Re11 + 3, or with PBS, were intranasally challenged with 10^5 50% egg infective doses (EID_{50}) of the indicated virus. These challenged birds were monitored for disease symptoms and mortality for two weeks following the challenge. Oropharyngeal and cloacal swabs were collected on days 3 and 5 p.c. to detect the presence of the virus in 10-day-old embryonated eggs. All the chickens were euthanized by CO_2 at the end of the experiment.

Statistical analysis

The raw data obtained from the samples were transformed to a logarithmic scale prior to conducting further analysis. To evaluate the statistical significance between distinct groups, the Unpaired *t*-test was employed using GraphPad Prism (v8) software, assuming that both populations have an identical standard deviation (SD). A p-value of less than 0.05 was considered statistically significant.

Data availability

All data pertaining to this study are available within the main body of this paper or in the Supplementary Materials section. Additionally, the resources, data, and reagents utilized in this study can be obtained from the corresponding author upon reasonable request.

Received: 1 April 2024; Accepted: 6 August 2024;
Published online: 19 August 2024

References

1. Yoon, S. W., Webby, R. J. & Webster, R. G. Evolution and ecology of influenza A viruses. *Curr. Top. Microbiol. Immunol.* **385**, 359–375 (2014).
2. Webster, R. G., Bean, W. J., Gorman, O. T., Chambers, T. M. & Kawaoka, Y. Evolution and ecology of influenza A viruses. *Microbiol Rev.* **56**, 152–179 (1992).
3. Tong, S. et al. New world bats harbor diverse influenza A viruses. *PLoS Pathog.* **9**, e1003657 (2013).
4. Tong, S. et al. A distinct lineage of influenza A virus from bats. *Proc. Natl. Acad. Sci. USA* **109**, 4269–4274 (2012).
5. Shi, J. et al. H7N9 virulent mutants detected in chickens in China pose an increased threat to humans. *Cell Res.* **27**, 1409–1421 (2017).
6. Shi, J., Zeng, X., Cui, P., Yan, C. & Chen, H. Alarming situation of emerging H5 and H7 avian influenza and effective control strategies. *Emerg. Microbes Infect.* **12**, 2155072 (2023).
7. World Health Organization. Avian Influenza Weekly Update Number 928. https://cdn.who.int/media/docs/default-source/wpro---documents/emergency/surveillance/avian-influenza/ai_20240105.pdf?sfvrsn=5f006f99_124#:~:text=To%20date%2C%20a%20total%20of,date%20of%2020%20October%202023 (2023).
8. Wei, C. J. et al. Next-generation influenza vaccines: opportunities and challenges. *Nat. Rev. Drug Discov.* **19**, 239–252 (2020).
9. Darricarrere, N. et al. Development of a pan-H1 influenza vaccine. *J Virol*. https://doi.org/10.1128/JVI.01349-18 (2018).
10. Chiba, S., Kong, H., Neumann, G. & Kawaoka, Y. Influenza H3 hemagglutinin vaccine with scrambled immunodominant epitopes elicits antibodies directed toward immunosubdominant head epitopes. *mBio* **14**, e0062223 (2023).
11. Arevalo, C. P. et al. A multivalent nucleoside-modified mRNA vaccine against all known influenza virus subtypes. *Science* **378**, 899–904 (2022).
12. Wong, T. M. et al. Computationally optimized broadly reactive hemagglutinin elicits hemagglutination inhibition antibodies against a panel of H3N2 influenza virus cocirculating variants. *J Virol*. https://doi.org/10.1128/JVI.01581-17 (2017).
13. Ping, X. et al. Generation of a broadly reactive influenza H1 antigen using a consensus HA sequence. *Vaccine* **36**, 4837–4845 (2018).
14. Giles, B. M. & Ross, T. M. A computationally optimized broadly reactive antigen (COBRA) based H5N1 VLP vaccine elicits broadly reactive antibodies in mice and ferrets. *Vaccine* **29**, 3043–3054 (2011).
15. Elliott, S. T. C. et al. A synthetic micro-consensus DNA vaccine generates comprehensive influenza A H3N2 immunity and protects mice against lethal challenge by multiple H3N2 viruses. *Hum. Gene Ther.* **29**, 1044–1055 (2018).
16. Carter, D. M. et al. Design and characterization of a computationally optimized broadly reactive hemagglutinin vaccine for H1N1 influenza viruses. *J. Virol.* **90**, 4720–4734 (2016).
17. Chen, M. W. et al. Broadly neutralizing DNA vaccine with specific mutation alters the antigenicity and sugar-binding activities of influenza hemagglutinin. *Proc. Natl. Acad. Sci. USA* **108**, 3510–3515 (2011).
18. Wiley, D. C. & Skehel, J. J. The structure and function of the hemagglutinin membrane glycoprotein of influenza virus. *Annu. Rev. Biochem.* **56**, 365–394 (1987).
19. Knossow, M., Daniels, R. S., Douglas, A. R., Skehel, J. J. & Wiley, D. C. Three-dimensional structure of an antigenic mutant of the influenza virus haemagglutinin. *Nature* **311**, 678–680 (1984).
20. Wiley, D. C., Wilson, I. A. & Skehel, J. J. Structural identification of the antibody-binding sites of Hong Kong influenza haemagglutinin and their involvement in antigenic variation. *Nature* **289**, 373–378 (1981).
21. Webster, R. G. & Laver, W. G. Determination of the number of nonoverlapping antigenic areas on Hong Kong (H3N2) influenza virus hemagglutinin with monoclonal antibodies and the selection of variants with potential epidemiological significance. *Virology* **104**, 139–148 (1980).
22. Caton, A. J., Brownlee, G. G., Yewdell, J. W. & Gerhard, W. The antigenic structure of the influenza virus A/PR/8/34 hemagglutinin (H1 subtype). *Cell* **31**, 417–427 (1982).
23. Gerhard, W., Yewdell, J., Frankel, M. E. & Webster, R. Antigenic structure of influenza virus haemagglutinin defined by hybridoma antibodies. *Nature* **290**, 713–717 (1981).
24. Kong, H. et al. Plasticity of the influenza virus H5 HA protein. *mBio*. https://doi.org/10.1128/mBio.03324-20 (2021).
25. Smith, D. J. et al. Mapping the antigenic and genetic evolution of influenza virus. *Science* **305**, 371–376 (2004).
26. Koel, B. F. et al. Antigenic variation of clade 2.1 H5N1 virus is determined by a few amino acid substitutions immediately adjacent

to the receptor binding site. *mBio* **5**, e01070–01014 (2014).
27. Broecker, F. et al. Immunodominance of antigenic site B in the hemagglutinin of the current H3N2 influenza virus in humans and mice. *J Virol*. https://doi.org/10.1128/JVI.01100-18 (2018).
28. Cai, Z., Zhang, T. & Wan, X. F. A computational framework for influenza antigenic cartography. *PLoS Comput. Biol.* **6**, e1000949 (2010).
29. Lapedes, A. & Farber, R. The geometry of shape space: application to influenza. *J. Theor. Biol.* **212**, 57–69 (2001).
30. Group, W. H. O. W. et al. Improving influenza vaccine virus selection: report of a WHO informal consultation held at WHO headquarters, Geneva, Switzerland, 14-16 June 2010. *Influenza Other Resp.* **7**, 52–53 (2013).
31. World Health Organization. Antigenic and genetic characteristics of zoonotic influenza A viruses and development of candidate vaccine viruses for pandemic preparedness. https://cdn.who.int/media/docs/default-source/influenza/who-influenza-recommendations/vcm-southern-hemisphere-recommendation-2022/202110_zoonotic_vaccinevirusupdate.pdf?sfvrsn=8f87a5f1_1 (2023).
32. Tian, J. et al. Highly pathogenic avian influenza virus (H5N1) clade 2.3.4.4b introduced by wild birds, China, 2021. *Emerg. Infect. Dis.* **29**, 1367–1375 (2023).
33. Zeng, X. et al. Protective efficacy of an H5N1 inactivated vaccine against challenge with lethal H5N1, H5N2, H5N6, and H5N8 influenza viruses in chickens. *Avian Dis.* **60**, 253–255 (2016).
34. Zeng, X. Y. et al. Protective efficacy of an H5/H7 trivalent inactivated vaccine produced from Re-11, Re-12, and H7-Re2 strains against challenge with different H5 and H7 viruses in chickens. *J. Integr. Agr.* **19**, 2294–2300 (2020).
35. Zeng, X. Y. et al. Protective efficacy of an H5/H7 trivalent inactivated vaccine (H5-Re13, H5-Re14, and H7-Re4 strains) in chickens, ducks, and geese against newly detected H5N1, H5N6, H5N8, and H7N9 viruses. *J. Integr. Agr.* **21**, 2086–2094 (2022).
36. Cui, P. F. et al. Genetic and biological characteristics of the globally circulating H5N8 avian influenza viruses and the protective efficacy offered by the poultry vaccine currently used in China. *Sci. China Life Sci.* **65**, 795–808 (2022).
37. Fouchier, R. A. & Smith, D. J. Use of antigenic cartography in vaccine seed strain selection. *Avian Dis.* **54**, 220–223 (2010).
38. Cui, P. et al. Global dissemination of H5N1 influenza viruses bearing the clade 2.3.4.4b HA gene and biologic analysis of the ones detected in China. *Emerg. Microbes Infect.* **11**, 1693–1704 (2022).
39. Gu, W. et al. Novel H5N6 reassortants bearing the clade 2.3.4.4b HA gene of H5N8 virus have been detected in poultry and caused multiple human infections in China. *Emerg. Microbes Infect.* **11**, 1174–1185 (2022).
40. Wilson, I. A., Skehel, J. J. & Wiley, D. C. Structure of the haemagglutinin membrane glycoprotein of influenza virus at 3 A resolution. *Nature* **289**, 366–373 (1981).
41. Popova, L. et al. Immunodominance of antigenic site B over site A of hemagglutinin of recent H3N2 influenza viruses. *PLoS One* **7**, e41895 (2012).
42. Wu, N. C. et al. Major antigenic site B of human influenza H3N2 viruses has an evolving local fitness landscape. *Nat. Commun.* **11**, 1233 (2020).
43. Li, J. et al. Amino acid substitutions in antigenic region B of hemagglutinin play a critical role in the antigenic drift of subclade 2.3.4.4 highly pathogenic H5NX influenza viruses. *Transbound. Emerg. Dis.* **67**, 263–275 (2020).
44. Peng, Y., Zou, Y., Li, H., Li, K. & Jiang, T. Inferring the antigenic epitopes for highly pathogenic avian influenza H5N1 viruses. *Vaccine* **32**, 671–676 (2014).
45. Rockman, S. et al. Reverse engineering the antigenic architecture of the haemagglutinin from influenza H5N1 clade 1 and 2.2 viruses with fine epitope mapping using monoclonal antibodies. *Mol. Immunol.* **53**, 435–442 (2013).
46. Rudneva, I. A. et al. Antigenic epitopes in the hemagglutinin of Qinghai-type influenza H5N1 virus. *Viral Immunol.* **23**, 181–187 (2010).
47. Khurana, S. et al. Antigenic fingerprinting of H5N1 avian influenza using convalescent sera and monoclonal antibodies reveals potential vaccine and diagnostic targets. *PLoS Med.* **6**, e1000049 (2009).
48. Kaverin, N. V. et al. Epitope mapping of the hemagglutinin molecule of a highly pathogenic H5N1 influenza virus by using monoclonal antibodies. *J. Virol.* **81**, 12911–12917 (2007).
49. Xu, N. et al. Emerging of H5N6 subtype influenza virus with 129-glycosylation site on hemagglutinin in poultry in China acquires immune pressure adaption. *Microbiol. Spectr.* **10**, e0253721 (2022).
50. Hu, Y. F. et al. Rational design of a booster vaccine against COVID-19 based on antigenic distance. *Cell Host Microbe* **31**, 1301–1316 e1308 (2023).
51. Lu, X. et al. Cross-protective immunity in mice induced by live-attenuated or inactivated vaccines against highly pathogenic influenza A (H5N1) viruses. *Vaccine* **24**, 6588–6593 (2006).
52. Govorkova, E. A., Webby, R. J., Humberd, J., Seiler, J. P. & Webster, R. G. Immunization with reverse-genetics-produced H5N1 influenza vaccine protects ferrets against homologous and heterologous challenge. *J. Infect. Dis.* **194**, 159–167 (2006).
53. Cao, Z. et al. The epitope and neutralization mechanism of AVFluIgG01, a broad-reactive human monoclonal antibody against H5N1 influenza virus. *PLoS One* **7**, e38126 (2012).
54. Gu, C. et al. Glycosylation and an amino acid insertion in the head of hemagglutinin independently affect the antigenic properties of H5N1 avian influenza viruses. *Sci. China Life Sci.* **62**, 76–83 (2019).
55. Meng, F. et al. A Eurasian avian-like H1N1 swine influenza reassortant virus became pathogenic and highly transmissible due to mutations in its PA gene. *Proc. Natl. Acad. Sci. USA* **119**, e2203919119 (2022).
56. Kong, H. H. et al. H3N2 influenza viruses with 12-or 16-amino acid deletions in the receptor-binding region of their hemagglutinin protein. *mBio*. **12**, e0151221 (2021).
57. Fonville, J. M. et al. Antibody landscapes after influenza virus infection or vaccination. *Science* **346**, 996–1000 (2014).

Acknowledgements

This study was supported by the National Natural Science Foundation of China (32172837), the National Key Research and Development Program of China (2021YFD1800201), by the National Natural Science Foundation of China (32202798), the National Key Research and Development Program of China (2022YFD1801200 and 2021YFC2301700), the Innovation Program of Chinese Academy of Agricultural Sciences, Innovation Program of Chinese Academy of Agricultural Sciences (Grant number CAAS CSLPDCP-202301), and the Central Public-interest Scientific Institution Basal Research Fund (1610302022017).

Author contributions

H.C., G.D., H.K., and Y.Z. conceptualized and designed the study. Y.Z., P.C., J.S., X.Z., Y.J., Y.C., J.Z., C.W., Y.W., and G.T. performed the experiments. J.S., X.Z., C.W., Y.W., Y.C., G.T., and Y.J. participated in animal immunizations and infections. All authors have examined and validated the contents of the manuscript.

Competing interests
The authors declare no competing interests.

Additional information
Supplementary information The online version contains supplementary material available at https://doi.org/10.1038/s41541-024-00947-4.

Correspondence and requests for materials should be addressed to Huihui Kong or Guohua Deng.